Brain and Cognition 85 (2014) 259–270

Contents lists available at ScienceDirect

Brain and Cognition

journal homepage: www.elsevier.com/locate/b&c

A model of curved saccade trajectories: Spike rate adaptation in the brainstem as the cause of deviation away

Wouter Kruijne [a,*], Stefan Van der Stigchel [b], Martijn Meeter [a]

[a] Cognitive Psychology, Faculty of Psychology and Education, Vrije Universiteit Amsterdam, Van der Boechorststraat 1, 1081 BT Amsterdam, The Netherlands
[b] Experimental Psychology, Helmholtz Institute, Utrecht University, Heidelberglaan 2, 3584 CS Utrecht, The Netherlands

ARTICLE INFO

Article history:
Accepted 7 January 2014
Available online 30 January 2014

Keywords:
Saccade deviation
Curvature
Superior colliculus
Brainstem
Spike rate adaptation
Long lead burst neurons

ABSTRACT

The trajectory of saccades to a target is often affected whenever there is a distractor in the visual field. Distractors can cause a saccade to deviate towards their location or away from it. The oculomotor mechanisms that produce deviation towards distractors have been thoroughly explored in behavioral, neurophysiological and computational studies. The mechanisms underlying deviation away, on the other hand, remain unclear. Behavioral findings suggest a mechanism of spatially focused, top-down inhibition in a saccade map, and deviation away has become a tool to investigate such inhibition. However, this inhibition hypothesis has little neuroanatomical or neurophysiological support, and recent findings go against it. Here, we propose that deviation away results from an unbalanced saccade drive from the brainstem, caused by spike rate adaptation in brainstem long-lead burst neurons. Adaptation to stimulation in the direction of the distractor results in an unbalanced drive away from it. An existing model of the saccade system was extended with this theory. The resulting model simulates a wide range of findings on saccade trajectories, including findings that have classically been interpreted to support inhibition views. Furthermore, the model replicated the effect of saccade latency on deviation away, but predicted this effect would be absent with large (400 ms) distractor-target onset asynchrony. This prediction was confirmed in an experiment, which demonstrates that the theory both explains classical findings on saccade trajectories and predicts new findings.

1. Introduction

Because of the limited resolution of the retina outside of the fovea, visual perception relies on a stream of rapid eye movements to fixate locations of interest. These eye movements (saccades) are intended to bring the fovea from one location to the next, yet almost never follow a straight line; they are usually curved. Some of this curvature is idiosyncratic to the observer, and some of it seems to be unsystematic noise (Optican and Robinson, 1980). However, curvature is also partly influenced by cognitive factors. In particular, saccade deviation from the optimal path is known to be affected by the presence of non-target elements in the visual scene, so-called distractors. (Van der Stigchel, 2010; Van der Stigchel et al., 2006).

1.1. Saccade deviation, population coding and inhibition

To study curved saccades, a distractor paradigm (Sheliga et al., 1994; Doyle and Walker, 2001) is often used: observers make a speeded saccade to a predefined target as soon as it appears, and a distractor (or more rarely, several) appears in the scene simultaneously with the target. When the distractor appears close to the target (Walker et al., 1997, within 20°), saccades will tend to deviate[1] towards the distractor. This may result in so-called 'global-effect' saccades, where the gaze lands in the middle between target and distractor. (Coren and Hoenig, 1972; Van der Stigchel and Nijboer, 2011).

In explaining these deviations, it is commonly assumed that the oculomotor system utilizes a saccade map where spatially organized activity is evoked by stimuli. To determine the saccade goal, stimuli compete for selection by means of lateral inhibition, where the losing location is suppressed and the remaining target activity is translated into a motor command. The oculomotor pathway indeed contains multiple structures that could implement such a visuomotor map, and of particular interest is the superior colliculus (SC). The SC is a layered midbrain structure, and its intermediate

* Corresponding author.
E-mail address: w.kruijne@vu.nl (W. Kruijne).

[1] Different studies on saccadic behavior have used variable measures and terminology to characterize saccade trajectories. Throughout this article, 'deviation' is used to indicate the angle between the initial direction of the saccade and a straight line from the starting point to the target. 'Curvature' is used whenever we want to emphasize the trajectory of the saccade, which usually displays a decrease in deviation as the saccade curves back towards the target mid-flight.

0278-2626/$ - see front matter © 2014 Elsevier Inc. All rights reserved.
http://dx.doi.org/10.1016/j.bandc.2014.01.005

layers (a) implement a retinotopic map in which activity in visuomotor neurons corresponds to the current visual input (Robinson, 1972; Marino et al., 2008); (b) are known to trigger saccades in response to sufficient stimulation, directed to the location of receptive visual field at the stimulated location (Robinson, 1972; Gandhi and Katnani, 2011); (c) integrate dense projections from striate, extrastriate and frontal areas that all implement retinotopic representations (Munoz and Schall, 2004, chap. 3; Schlag-Rey et al., 1992; Sommer and Wurtz, 2000); and (d) constitute the primary source of input for the brainstem burst neurons that drive the eye muscles (Sparks, 2002; Scudder et al., 2002). The central role of the SC in saccade generation is illustrated in Fig. 1a.

Deviation towards and the global effect are well explained in terms of population coding in this map (Lee et al., 1988): when distractor activity is not suppressed completely before the saccade, it contributes to the movement which might then deviate to an intermediate location, and land there as well. This explanation is supported by the findings that simultaneous electrical stimulation at two collicular locations results in averaging saccades (Katnani et al., 2012; Robinson, 1972), and that SC recordings during visually evoked averaging saccades are marked by distributed peaks at short latencies, and activity at an intermediate location for longer latency-saccades (Edelman and Keller, 1998; Glimcher and Sparks, 1993). Various successful computational explorations of this theory have been developed (Arai et al., 1994; Trappenberg et al., 2001; Meeter et al., 2010).

In humans, there is also a set of conditions that make saccades consistently deviate away from distractors. The currently dominant interpretation of deviation away from distractors relies on extending the population coding view with spatially focused distractor inhibition in the saccade map. Excessive suppression of the distractor location would 'deflect' the motor command to the opposite direction, and cause the saccade to deviate away (Godijn and Theeuwes, 2002; McSorley et al., 2004; Van der Stigchel, 2010; Walker and McSorley, 2008). Evidence for such spatial inhibition is mostly behavioral, and can be summarized as these effects:

- The *latency effect* refers to an often found correlation between deviation away and saccadic latency (McSorley et al., 2006; Mulckhuyse et al., 2009; Ludwig and Gilchrist, 2003), with more deviation away occurring for long-latency saccades. This is then interpreted as attentional inhibition building up over time, mostly affecting saccades with long latencies.
- The distractor *similarity effect* has been reported (Ludwig and Gilchrist, 2003; Mulckhuyse et al., 2009), a finding that distractors similar to the target cause more deviation towards at short latencies than very dissimilar stimuli, yet at longer latencies similar distractors evoke more deviation away. The interpretation is that similar distractors require more and stronger inhibition, but that this inhibition is later than with dissimilar – more easily dissociable – distractors.
- Distractor location is known to affect deviation, with greater angular target-distractor distances, or smaller fixation-distractor distances inducing more deviation away (McSorley et al., 2009a; Van der Stigchel et al., 2007). This *position effect* is often explained through the locus of inhibition in the map: in both cases, inhibition has a larger spatial effect on the initial trajectory of the saccade, resulting in greater deviation away.
- Apart from these exogenous manipulations, several *endogenous effects* have been reported: merely expecting a stimulus to appear, or maintaining a location in working memory can result in deviation away without physical distractors (Godijn and Theeuwes, 2004; Van der Stigchel and Theeuwes, 2006; Theeuwes et al., 2009). Explanations of such findings rely on tenets that endogenous processes like attention and working memory will automatically activate representations in the (oculo) motor system (Rizzolatti et al., 1987; Sheliga et al., 1994; Postle, 2006), which in turn yields similar suppression effects.

From such findings it is often concluded that saccade deviation can be used to probe inhibition in the oculomotor system (McSorley et al., 2006; Van der Stigchel et al., 2006; Theeuwes et al., 2009): the amount and direction of saccadic deviation is taken as a measure of inhibition produced by attention mechanisms. However, strong neuroanatomical or neurophysiological evidence for this view is lacking, and to our knowledge no computational model has thus far successfully incorporated this theory, despite its apparent simplicity. Top-down inhibition has therefore functioned more or less as a deus ex machina, called upon to explain deviation away when it occurs, yet remaining unexplained itself.

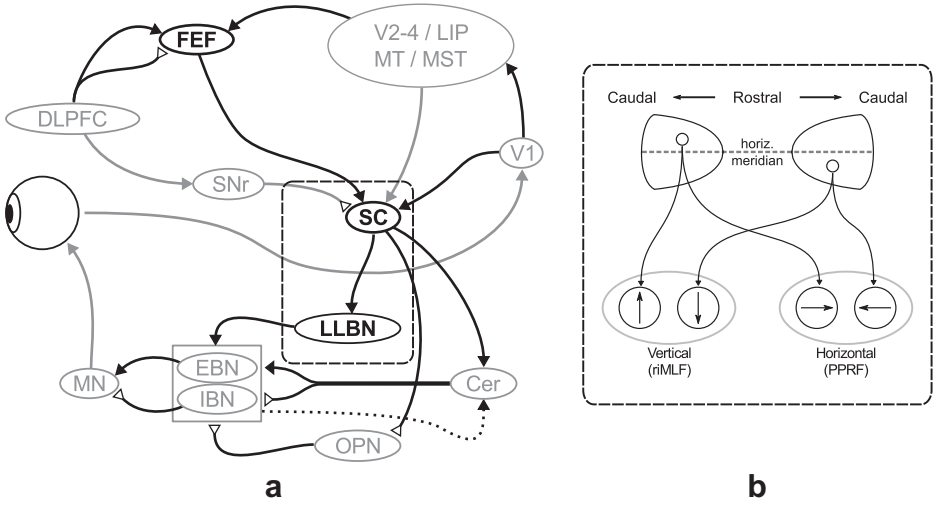

Fig. 1. (a) Schematic representation of the oculomotor system. Markers indicate whether connections are excitatory (solid triangle: ▼) or inhibitory (inverted open triangle: △). Only structures and connections in black are explicitly represented in our model, those in gray are not. See the text for the abbreviations and more detail. (b) Detailed excerpt of the projection from SC to LLBN in (a), schematically outlining how retinotopically organized SC-output is decomposed into the vectorial representation maintained in the brainstem. For two representative neurons in the SC, it is shown how their output is decomposed into directional components for vertical and horizontal eye movements. For example, the top left SC-neuron represents a location in the upper right visual field. Activity at this location projects to brainstem neurons that code for upwards and for rightwards movement. The relative strength of these connections determines the balance between these two components, so that together they produce a movement vector in the appropriate direction.

Moreover, an increasing body of findings from the literature seem to strongly challenge the theory, as reviewed below.

1.2. Challenges to the spatial top-down inhibition theory

Although the behavioral effects mentioned above seem to converge on a spatial top-down inhibition view of saccade deviation, there are several reasons to challenge the view. First, extensive research on the anatomy and connectivity of the oculomotor system and the SC in particular (White et al., 2011, chap. 11; Munoz and Schall, 2004) has yielded remarkably little evidence for spatial inhibition. As Fig. 1a illustrates, projections to the SC are primarily excitatory. Only the substantia nigra pars reticulata (SNr) provides inhibition, but this is tonic and globally inhibits the SC. Saccades are preceded by a temporary release of this inhibition, which is centered around the target, but note that this spatial code is very coarse, and has a net excitatory effect (Jiang et al., 2003; Hikosaka et al., 2000). There thus seems to be no candidate source of spatial inhibition.

Secondly, White et al. (2012) were recently able to evoke deviation away in macaque monkeys and investigated the associated responses in the SC. In their study, the irrelevant distractor was presented either 400 ms before target onset (i.e. a distractor-target onset asynchrony; $DTOA_{400ms}$) or simultaneously ($DTOA_{0ms}$). The spatial inhibition view would predict that, in particular with $DTOA_{400ms}$, the magnitude of deviation away would depend on inhibition and would be predicted by the amount of activity at the distractor location after presentation. However, only 30 ms before saccade initiation did distractor activity somewhat predict deviation away, and in the $DTOA_{400ms}$ condition, no correlation was found for the critical 400 ms interval. This suggests that the distractor location was not being inhibited in this interval.

Thirdly, it is of note that the SC encodes locations rather than the trajectories to get there. This means that the characteristic 'curvature' that follows deviation away cannot result from one command to the brainstem, but must result from a correction signal that affects the trajectory mid-saccade. In line with this dissociation, the distractor location seems to affect the size of the initial deviation, but not the point of peak deviation (Van der Stigchel et al., 2007), and the shape of curvature is relatively unaffected by the initial deviation, even when the distractor is in the opposite hemifield (Doyle and Walker, 2001). The proposed source for this correction signal is the cerebellum, receiving inputs from the SC, and manipulating the brainstem activity in-flight (McSorley et al., 2004; Scudder et al., 2002; Quaia et al., 1999). This does however raise the question how the cerebellum can identify the proper target location when the SC cannot. If, for example other oculomotor areas were unaffected by inhibition and underly this corrective signal (McSorley et al., 2004), the result of this correction, negating inhibition effects, should be observed in SC as well, as these areas project there more densely (Munoz and Schall, 2004). Alternatively, the SC itself could complete target selection mid-saccade and drive correction, but this would suggest that with long latencies, complete selection should occur before saccade initiation; rather, these saccades are marked by more, rather than less deviation away.

In summary, it seems difficult to justify the assumption that inhibition accounts for saccade trajectories deviating away from distractors. To be precise, we do not claim that inhibition does not play any role in target selection in the oculomotor system, but a mechanism of excessive spatial inhibition of distractors is clearly at odds with the findings discussed here, as was similarly inferred by White et al. (2012). Therefore, we propose a novel theory in this article that suggests that deviation away does not rely on inhibitory signals but originates downstream, in the vectorial command encoded by the brainstem.

1.3. An adaptation theory of deviation away

The SC is often considered the 'final stage' of oculomotor competition, and it is where most retinotopically organized signals converge and are translated into a brainstem command that controls the eye muscles. This command has a vectorial representation (Fig. 1b) where neurons encode horizontal and vertical displacement by a rate code, where firing rates encode the velocity and length of the saccade (Van Gisbergen et al., 1981; Sparks, 2002). Coarsely, the paramedian pontine reticular formation (PPRF) has neurons that encode the horizontal component, whereas the rostral interstitial nucleus of the medial longitudinal fasciculus (riMLF) encodes vertical movement.

For both components similar neurons have been identified that comprise the pathway (Fig. 1a) from the SC to the Motor Neurons (MNs). The SC projects to the long-lead burst neurons (LLBNs), which after stimulus onset show increased activity leading to a burst some 80–30 ms before the saccade (Scudder et al., 1996; Rodgers et al., 2006). The LLBNs then seem to serve as a relay, projecting onto the excitatory and inhibitory burst neurons (EBNs/IBNs) (Ramat et al., 2007; Sparks, 2002). These are characterized by a burst shortly before saccade onset, and project to MNs in coordinated fashion: EBNs excite the MNs that tense the muscles in the desired direction, and simultaneously the opposing MNs are inhibited by IBN (Van Gisbergen et al., 1981; Ramat et al., 2007; Sparks, 2002). The EBNs/IBNs are also directly innervated by the SC (Scudder et al., 2002).

To prevent that all SC-activity will immediately activate this purely excitatory pathway and evoke an eye movement, the EBNs/IBNs receive tonic inhibition from the omnipause neurons (OPNs) (Evinger et al., 1982; Ramat et al., 2007). OPNs are located in the midline pons and inhibit burst neurons regardless of preferred direction. A saccade onset is marked by a sudden pause in OPN activity, which is reinstated once the saccade is terminated. Early findings suggested a prominent role for the SC, with its fixation neurons in particular, in regulating OPN activity (Gandhi and Keller, 1997), but more recent evidence suggests other sources may contribute to the initiation of the OPN-pause that results in saccades (Jantz et al., 2013; Gandhi and Keller, 1999; Everling et al., 1998). Although the OPN-pause seems to mark saccade initiation, they do not seem to terminate saccades (Rodgers et al., 2006; Rucker et al., 2011).

In general, projections within the SC–MNs pathway seem to be either excitatory or direction-unspecific, which makes it unlikely that inhibition within this pathway could readily explain saccadic curvature. Note, however, that the OPNs do not suppress LLBN-activity (Rodgers et al., 2006; Sparks, 2002; Scudder et al., 2002; Ramat et al., 2007). We thereby infer that throughout target selection preceding saccade initiation, LLBNs will already respond to SC-activation evoked by both the distractor and the target. Studies on averaging express saccades show that the movement vector resulting from activity at these sites will point to an intermediate location (Edelman and Keller, 1998). It seems reasonable to assume that these initial signals could induce spike rate adaptation, a general property of the brain where the firing rate of a neuron decreases after prolonged stimulation (Barlow, 1961). Spike rate adaptation can result from various different processes, such as accommodation of the postsynaptic membrane, after-spike hyper-polarization (AHP), or synaptic depletion. We propose, without appointing a specific underlying mechanism, that adaptation is the primary cause of deviation away.

Consider, for example, the case that a rightward target and a distractor at a 45° angle in the upper hemifield are presented (see Fig. 2b). Both representations stimulate the LLBNs and a prematurely initiated saccade would deviate toward the distractor. If no saccade is initiated, competition eventually selects the target

and due to lateral inhibition distractor activity eventually falls to baseline. Distractor activity would have left a trace however, in the form of adaptation in the brainstem, rendering the upwards LLBNs less sensitive than the opposite direction. This results in an unbalanced saccade command biased away from the distractor (Fig. 2c). This asymmetry then results in deviation away. Notably, this directional unbalance is present solely at the brainstem level, and the SC still holds the desired correct landing position for the saccade. The resulting mismatch between the SC representation and the LLBN-drive could then determine the corrective signal that steers the saccade back to the intended target mid-flight, possibly mediated by the cerebellum.

With a somewhat higher-level description, this adaptation theory emphasizes three dissociable processes in producing a saccade. The process of target *selection* takes place in the spatially organized oculomotor pathway converging onto the SC, and is thus largely reflected there (Ramat et al., 2007). The SC output determines the *drive*, the vectorial command in the brainstem relayed through the LLBNs (Sparks, 2002). The third process *correction*, is initiated mid-saccade, and depends on comparing the drive to the selection. This is a process most likely mediated by the cerebellum (Optican and Robinson, 1980). A notable feature of the adaptation theory is that it identifies different processes underlying deviation towards and deviation away: deviation towards is due to unsuccessful selection, and deviation away arises in the drive. Note, however, that despite this difference, the theory still implies a continuum from deviation towards to deviation away, as the direction and magnitude of deviation are determined by the balance between distractor activation at saccade onset and preceding distractor activation. This is supported by the data from White et al. (2012) where distractor activity was slightly larger at the moment of saccade initiation for saccades deviating towards than those deviating away, yet only at the moment of saccade initiation, and not earlier. Previous recordings in the SC and frontal eye fields (FEF) have yielded similar findings (McPeek et al., 2003; McPeek, 2006).

In understanding how adaptation gives rise to the observed modulatory effects on deviation away, we stress that independent of the underlying mechanism, two main factors determine the magnitude of adaptation, namely strength and duration of the preceding stimulation: stronger and longer stimulation produce larger adaptation effects. However, it seems reasonable to assume that adaptation will saturate and will never render neurons completely unresponsive. In oculomotor selection, strength and duration of stimulation will rarely be unrelated: as stronger distractor signals should generally lengthen the selection process yielding more profound adaptation. Taken together, this makes that adaptation can well account for effects on deviation away.

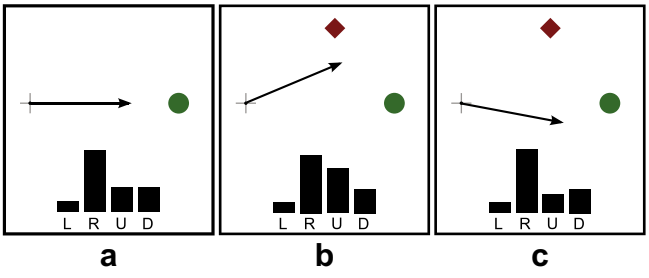

Fig. 2. Proposed mechanism producing deviation away, illustrated for a rightward saccade. (a) With a single target (circle), LLBN activity (black bars for all four directions) is most prominent to the right but does involve smaller, balanced components up and down. (b) When a target and a distractor (diamond) are presented, both elicit LLBN-activity. The resulting saccade command (involving both large upwards and rightwards components) points to a location between them (compare to activity in (a)). (c) When a saccade is made after the target has been successfully selected and distractor activity has been inhibited, the saccade command is similar to (a), as there is no more additional stimulation of the upwards component by the distractor. However, past activity in this component has lead to adaption, which causes these neurons to fire less than those coding for the downwards component. The resulting unbalanced command leads to deviation away from the distractor.

- The *latency effect* is accounted for in two ways: first, due to incomplete selection with short-latency saccades, the likelihood of deviation towards distractors is higher with short latency saccades, whereas with long latency saccades, adaptation effects will likely be larger than residual distractor activation. Secondly, long latencies are more likely to occur when selection is difficult, thus when distractor stimulation was stronger and evoked stronger adaptation effects.
- The *similarity effect* is closely related to the latency effect (Ludwig and Gilchrist, 2003). More similar stimuli suggest a longer phase of unresolved competition, which would explain why similar distractors evoke deviation towards for fast saccades, and stronger deviation away for long-latency saccades.
- The explanation for the *position effect*, that larger angular distance between the target and distractor tends to evoke larger deviation away, is again driven by two factors: with distractor and target in close proximity, selection is more likely to fall short and evoke a global effect, plus with an increasingly larger angle, decomposition of distractor activity has a larger pulse in the direction perpendicular to the target, thereby producing larger deviation away.
- In explaining the *endogenous effects* the adaptation theory relies on the same tenets as inhibition theories, namely that attending or memorizing locations would activate the oculomotor system in the presaccadic interval similar to how a physical distractor would. Indeed, SNr and Lateral Intraparietal (LIP) activity during, for example, delayed saccades provides evidence for such endogenously induced SC activation (Handel and Glimcher, 2000; Brown et al., 2004; Ferraina et al., 2002). However, the adaptation theory abolishes the need for additional inhibition at that location.

The adaptation theory offers an explanation for these well-established effects on deviation away that can still be reconciled with the challenges faced by inhibition theories. Coincidentally, the notion that these effects have generally been attributed to inhibition in the selection process is indicative of the complexity of disentangling the two theories. They differ in the locus of the source of deviation away, but it seems impossible to stimulate the brainstem drive without affecting the selection process in the SC in vivo. For example, modulating distractor intensity could affect adaptation in the brainstem, but such a manipulation will similarly affect timing and strength of SC responses (Bell et al., 2006). If this were then shown to affect deviation, the 'deus ex machina'-nature of inhibition theories would always allow for an explanation of this effect in terms of stronger evoked inhibition.

However, the adaptation theory makes a specific prediction regarding the latency effect in the DTOA-paradigm introduced by White et al. (2012). Because the adaptation theory poses that deviation away depends on past distractor activity, and because this is expected not to vary all too much between trials during the persistent presence of a stimulus, the theory predicts that this correlation should be absent or at least much smaller with $DTOA_{400ms}$ than with $DTOA_{0ms}$. The inhibition theory, on the other hand, would only be reconcilable with the data from White et al. (2012) if inhibition were to operate *just* before saccade initiation, with as a result that the same inhibition induced latency effect would be found.

In this study, we first explore the feasibility of the adaptation theory through simulations with a neurocomputational model,

reimplementing that of Meeter et al. (2010), which already successfully simulated saccadic behavior in various paradigms, including latency distributions, the gap effect, antisaccade behavior, deviation towards distractors and global effect. We simulated different deviation-effects as well as our prediction for the DTOA-task. Following, we confirm our prediction experimentally by exploring eye movements from human observers in the DTOA paradigm.

2. Calculation

2.1. A neural model of the oculomotor system

In this section, we dissociate brain structures from their modeled counterparts with similar names by using bold-faced text for model structures. Our model is a reimplementation of (Meeter et al., 2010), largely maintaining their formalization of the target selection process, but implementing the drive- and correction processes conform the adaptation theory outlined above. This section is largely descriptive and more detail is provided in A.

2.1.1. Selection: SC input and the saccade map

The selection process was implemented by abstracting the neural pathway from visual input through the cortex converging onto the SC and competition within the SC itself. Literature on involved connections is relatively extensive and consistent (White et al., 2011; Munoz and Schall, 2004; Munoz, 2002; Lui et al., 1995), and identifies three distinct sources of SC-input (see also Fig. 1a): (1) The retina and V1 project to SC both directly and via its superficial layers. This evokes in a swiftly decaying visual pulse. (2) The cortical pathway from striate cortex to frontal areas receives input from these early areas as well and provides a delayed, more persistent input to the SC following stimulus presentation A key structure in this pathway seems to be the FEF, a structure that also implements topographically organized stimulus representations that compete for selection (Sommer and Wurtz, 2000), and projects densely onto the SC. An important difference between the two maps is that FEF not only integrates exogenous signals from visual areas, but also endogenous excitatory and inhibitory signals from other areas including the Dorsolateral Prefrontal Cortex (DLPFC) (Munoz, 2002) and LIP (Kusunoki et al., 2000) (These structures also project to the SC, yet strictly excitatory; Ferraina et al., 2002; Johnston and Everling, 2006). (3) The SNr in the basal ganglia circuitry modulates SC-activity through tonic inhibition. Upon target selection this inhibition is released, allowing competition within the SC (Basso and Wurtz, 2002). Its projections are spatially relatively coarsely coded (Jiang et al., 2003; Hikosaka et al., 2000).

The abstraction of exogenous input involved a **V1**-structure with separate input units for every stimulus on the display. Unit behavior was defined as a brief intense pulse following stimulus onset, persistent activity during stimulus presence, and slow exponential decay following offset (cf. Gawne and Martin, 2002). Endogenous influences were implemented similarly by a **DLPFC** input structure. The endogenous signal would trail **V1**-activity by 30 ms, rise linearly and would decay more slowly upon stimulus offsets (cf. Tinsley and Everling, 2002). Endogenous and exogenous inputs were integrated by an **FEF**-structure, which modeled unit activity by leaky integrate-and-fire units (LIF) with continuous firing rates. Endogenous distractor input was inhibitory, and lateral inhibition in **FEF** facilitated target selection. Deviating from the original implementation but in line with our theory, input to the **SC** was only excitatory, integrating inputs from **V1** and **FEF**.

The **SC** was implemented as two sheets of LIF-units, and grid positions were mapped to visual space through the coordinate system of Van Gisbergen et al. (1987). **SC**-inputs had Gaussian projections centered around the corresponding stimulus location, and lateral inhibition (Munoz and Istvan, 1998) was implemented by each node inhibiting all others. Parameters for the Gaussian projection and lateral inhibition were chosen to match estimates of the visual field size from SC-neurophysiology (Trappenberg et al., 2001; Dorris et al., 2007).

2.1.2. Drive and correction: LLBN and cerebellum

We have outlined that in the brainstem, a vectorial displacement command directs the saccade, primarily controlled by distributed SC-activity (Sparks, 2002). There is ongoing debate regarding how exactly SC-activity is decomposed into this command (Katnani et al., 2012; Gandhi and Katnani, 2011). In the model we chose a transformation based on simple vector summation: every node in the **SC** activates the brainstem, and the contribution of each node in each direction is determined by node output and the position of the corresponding visual field location. The resulting directional code was summarized by four values for the cardinal directions (up, down, left and right). Linear scaling of this decomposition determined the initiation, drive and the correction processes in a saccade.

The involvement of the SC in saccade initiation has often been shown, but it is still unclear to what extent other regions, including even downstream LLBNs might have a modulatory role in determining the OPN-pause (Jantz et al., 2013; Rodgers et al., 2006; Ramat et al., 2007). For simplicity, we implemented a straightforward fixed-threshold implementation (in line with Meeter et al., 2010) where a saccade was assumed to be initiated once the summed decomposed **SC** activity, opposing directions counteracting, crossed a certain value. Note that this also implied that similar stimulation at larger eccentricities would be faster to evoke saccades, which is at best only partially true and dependent on factors such as stimulus size, color and intensity (Dick et al., 2004; Kalesnykas and Hallett, 1994). Therefore all stimuli in our simulations (discussed below) had the same eccentricity.

In line with the relatively straightforward pathway from the SC to the MNs the decomposed **SC**-output directly determined the drive of the saccade conveyed by the brainstem. However, as the proposed locus of firing rate adaptation, four **LLBN**-units were modeled to relay the decomposed **SC** activity in the cardinal directions. To model adaptation, unit output v, was modulated by an accommodation factor u, where u was a moving average of the neuron's past activity v (Meeter et al., 2005; Izhikevich, 2003). During a saccade, **LLBN**-output v in all directions defined the drive.

The adaptation theory assumes SC-activity during the saccade reflects the intended displacement of the saccade, which is compared to the drive to determine the corrective signal. Most likely this is mediated by the cerebellum. The model shows how this correction signal can be determined from a simple computation (see Fig. 3) based on the current uncorrected drive and an efferent copy of the current eye position. The latter can be determined by integrating the burst neuron output. In the model, this was implemented by scaling the **LLBN** output vector and adding it to the eye position several time steps back (an efferent delay). The resulting extrapolated landing position was compared to the desired displacement from the **SC**, and the difference, scaled down, defined an appropriate corrective pulse. Notably, the resulting corrective signal not only gives rise to saccadic curvature, but also to the characteristic velocity profiles (Van Opstal and Goossens, 2008), as correction gradually slows down the saccade as well. Once the effective velocity drops to a prespecified low value, the saccade is considered terminated in the model. The resulting duration was approximately 35 ms for targets at 10°.

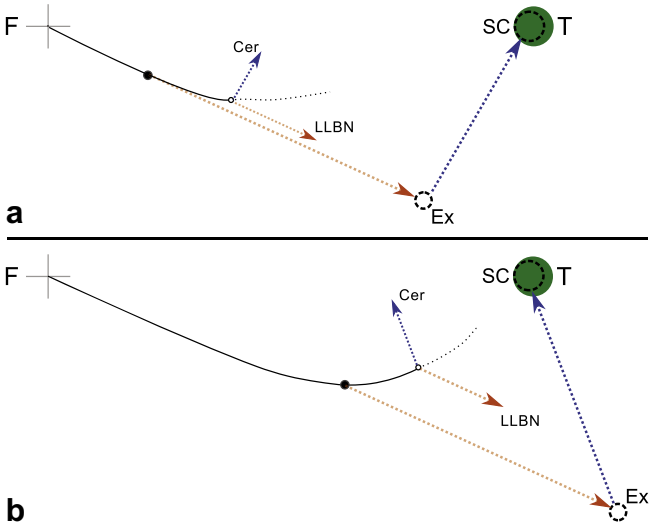

Fig. 3. Schematic representation of cerebellar correction during two saccades deviating away from a distractor in the upper visual field (not shown). F indicates the starting point, T indicates the target. The open circle marked SC indicates the saccade goal, as it is (correctly) represented in the SC. (a) The early phase of a deviating saccade (solid black line). The extrapolated landing position (Ex) of the saccade, if it went on uncorrected, is the result of adding the LLBN-based drive (LLBN) – scaled up – to the eye position estimated with an efferent delay, indicated by the filled dot on the saccade trajectory. The error between Ex and SC evokes a corresponding – scaled down – corrective signal (Cer), curving the trajectory back towards the goal. (b) The same computation at a later stage of a similarly deviating saccade. Here, a larger discrepancy between Ex and SC is found, both in direction and in eccentricity. The resulting cerebellar signal therefore produces curvature back to the target, but also corrects for the too large eccentricity of Ex and thereby slows down the saccade.

2.2. Model simulations

Saccades in several paradigms were simulated, all to a target located horizontally to the right at 10°. First, the compatibility of the reimplementation with the original model from Meeter et al. (2010) was explored by simulating the gap effect: a simple saccade to a single target stimulus, with fixation offset at $t = 0$ and a gap condition with offset at $t = -200$ (all times are reported with respect to target onset). The gap condition is expected to yield faster reaction times than the no-gap condition. To investigate the *position effect*, the distractor paradigm was modeled with the distractor at either 17°, 45° or 60° angular distance in the upper visual field; the first position was expected to result primarily in deviation towards, whereas further distances should produce increasingly large deviation away. The *latency effect* was explored for distractors at 17° and 45°. Finally, to test our predictions regarding the DTOA-paradigm, these distances were also simulated with the distractor at $t = -400$.

To study these effects, the latency effect in particular, a population of saccades with plausible internal variance in latency is needed. This was generated by varying the five model parameters that represented endogenous and exogenous input strength in **V1** (target, distractor and fixation) and **DLPFC** (target and distractor) for each simulated paradigm. These parameters had the same normal distribution in each modeled paradigm. The range of values for each parameter resulted in 12,150 parameter combinations, and probabilities of each parameter combination were assigned according to their distribution (B). Each parameter combination resulted in a saccade trajectory and latency. Much like in behavioral experiments, trials were discarded if the saccades they produced (1) were initiated too early to be evoked by the target, i.e. within 80 ms from target onset or earlier; (2) deviated too far from the target and did not land within 3° from it; or (3) were not evoked within the simulation time (400 ms from target onset).

Of the remaining trials, the associated likelihoods were used to determine expected values for latency and deviation, and determine their weighted correlation. The position effect was tested qualitatively, by comparing saccade trajectories for all distractor positions with the five most likely parameter combinations.

3. Materials and methods

To test our predictions for the DTOA-paradigm, regarding the latency effect in particular, we conducted an experiment with human observers. One difficulty in the experimental design is that with 400 ms DTOA, distractor onset consistently predicts the timing of target onset, which can be used as a warning signal and speed up latencies compared to $DTOA_{0ms}$. To produce comparable latencies to study its effect on deviation, our $DTOA_{0ms}$ condition therefore included a warning stimulus at fixation with the same timing.

3.1. Participants

Sixteen participants (18–27 years old, mean 22; 6 male), all naive to the purpose of the study, participated in the experiment. All had normal or corrected-to-normal visual acuity. Informed consent was obtained prior to the study, which was done in accordance with the guidelines of the Helsinki Declaration.

3.2. Apparatus

Participants performed the experiment in a sound-attenuated setting, viewing a display monitor from a distance of 68 cm. Eye movements were recorded by an Eyelink II system (SR Research Ltd., Canada), an infrared video-based eye tracker that has a 500 Hz temporal resolution, a spatial resolution of 0.01° and an accuracy $< 0.5°$. One participant was recorded with 250 Hz, but her data was in all regards similar to that of others so we did not exclude her. The participants' heads were stabilized with a chin rest, and an infrared remote tracking system compensated for any residual head motion. The left eye was monitored. An eye movement was considered a saccade when either eye velocity exceeded 35°/s or eye acceleration exceeded $9500°/s^2$.

3.3. Stimuli and design

All stimuli (fixation, target, distractor) were gray (85.63 cd/m^2) on a black background (1.15 cd/m^2). Each trial started with the presentation of a '+' character ($1.0° \times 1.0°$) in the center of the screen as the fixation stimulus.

In The $DTOA_{0ms}$-block, the fixation stimulus was replaced by a green (31.61 cd/m^2) fixation stimulus after 350 ms. After another 400 ms the target (a solid circle with 1.4° diameter) appeared at 8.4° eccentricity, either above, below, right or left from fixation. In one-fifth of the trials, the target was the only element presented. In the remaining trials, a diamond-shaped distractor (sides measuring $1.1° \times 1.1°$) appeared simultaneously, in one of the four quadrants, at 6.0° eccentricity. Both stimuli were presented for 1500 ms. In the $DTOA_{400ms}$-block, fixation remained gray but a distractor was always presented, 350 ms from fixation onset, followed by a target 400 ms later. Participants were instructed to fixate on the center of the screen, and make a single, accurate saccade to the target stimulus when it appeared, in both tasks. The $DTOA_{0ms}$-block consisted of a training session of 20 trials followed by 600 experimental trials; the $DTOA_{400ms}$-block had 16 practice-trials and 480

experimental trials. The trial sequence was randomized and block order was counterbalanced across participants.

3.4. Data analysis

Saccade latency was measured as the interval between target onset and saccade initiation. Trials were excluded when latencies were under 80 ms or over 600 ms, if no saccade was detected, or if the first saccade was too small ($< 3^\circ$). Trials were classified as errors and not analyzed if the saccade started more than 1.5° from the center of the fixation cross, or landed over 3° from the center of the target. For the remaining trials saccade deviation was defined by the mean angle of the trajectory compared to a straight line from the starting point of the saccade to the target, during the first 10 ms of the saccade (Van der Stigchel et al., 2006). Deviation was then compared to idiosyncratic deviation, measured from the trials without a distractor. Deviations were signed so that positive values indicate deviation towards, negative values away. A mean deviation of zero thus indicates no difference between the no-distractor and the distractor condition.

4. Results and discussion

4.1. Model results

Table 1 gives expected values for latency and deviation computed from the population of simulated saccades. Results for latencies indicate that the model produces realistically timed saccades and yields a clear gap effect of 50 ms much like the original model (Meeter et al., 2010). Of note, the latencies in the No Gap condition are relatively large compared to the 17° distractor condition. The literature indeed suggests that small distractor-target distances may speed saccades, (McSorley et al., 2009a; McSorley et al., 2009b), but others have reported comparable latencies for these two conditions (Walker et al., 1997). Likely, simultaneously presented stimuli compete throughout the visual cortex, which is not embedded in the model and could explain this difference. Nevertheless, the simulated latencies seem sufficiently realistic.

Saccade deviations, however, were our main interest. The results in Table 1 are in line with our theory: the 17° distractor conditions yield deviation towards, whereas deviation away was found in the 45° distractor configuration. The difference between those conditions, however, is notable: the magnitude of deviation away is much smaller than that of deviation towards. Such a difference has been shown in the literature (McSorley et al., 2009a). The discrepancy is more accentuated in the model because the size of deviation away in the model is relatively small. This might simply be the result of our LLBN-implementation, which was kept simple to focus on the core principles of adaptation theory. Moreover, too little data exists on these neurons to support more complex models. Trial models with more LLBN-units, more sophisticated projection mechanisms or broader SC-responses have yielded larger deviation away.

Unit behavior in the SC and upstream structure was much like that of Meeter et al. (2010) and implemented the selection process. Presaccadic activity in SC units was marked by a relatively small but early visual activity peak, followed by a more gradual rise after ≈ 70 ms. This second phase marked competition, where activity initially rose for both target- and distractor representation, but would then decay for the distractor while steeply increasing for the target.

The resulting drive, modeled as LLBN-output, clearly reflects this pattern. Fig. 4 depicts activity during an illustrative trial with deviation away. Activity in the 'rightwards'-node evolves in three phases: (1) the visual pulse in the SC evokes an early visual pulse in our simulated LLBN ($t = 70$ ms). Visual responses have been observed in the LLBNs, albeit relatively small (compare Munoz et al., 2000; Kaneko, 2006). Our model produces relatively large visual responses as it does not dissociate purely visual from visuomotor responses in the SC (Rodgers et al., 2006). (2) At about 100 ms before saccade initiation both target and distractor innervate the rightwards LLBN. Once distractor activity decays, there's a brief drop in rightwards activity, followed by (3) a steady increase of the response as the target representation rises in activity and governs the drive. Leftwards activity, on the other hand, remains

Table 1
Expected saccade latency and deviation in the model (i.e. mean value weighted by probability) in all simulated conditions.

Condition	Latency	Deviation
No gap	243.3	–
$Gap_{200\ ms}$	192.8	–
45° Distractor, $DTOA_{0ms}$	263.9	−0.26
17° Distractor, $DTOA_{0ms}$	208.3	7.5
45° Distractor, $DTOA_{400ms}$	260.1	−0.11
17° Distractor, $DTOA_{400ms}$	232.1	5.4

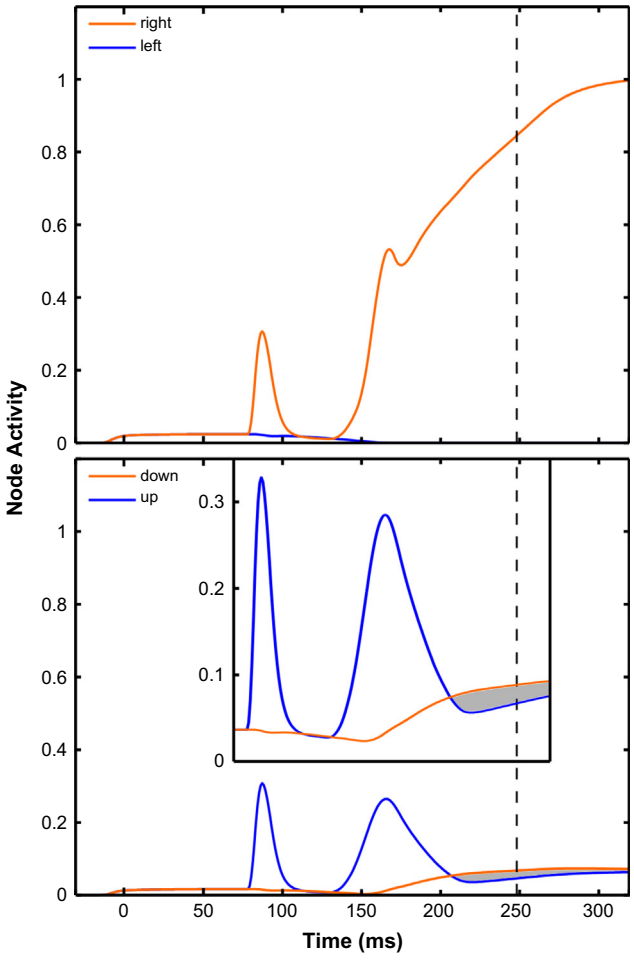

Fig. 4. Model LLBN-activity for a rightwards saccade deviating away from a distractor in the upper hemifield (−1.46°, latency = 279 ms). The dashed line marks LLBN-activity at saccade initiation. Top: right- and leftwards activity. Bottom: upwards and downwards activity. The distractor initially evokes upwards activity, which decays after the distractor loses competition. Due to adaptation, downwards activity consecutively surpasses upward activity at saccade initiation (shaded area). The inset shows the same pattern at a larger scale. 'Time' in this figure reflects time since stimulus onset, assuming a 70 ms time difference between stimulus onset and LLBN-innervation, and another 30 ms to traverse the brainstem pathway from LLBNs to motor neurons.

negligible. The two vertical components illustrate the adaptation effect: although both components are activate at saccade initiation, due to the distributed target representation, they are unbalanced. The upwards response evoked by the distractor in the preceding 100 ms has rendered this component less sensitive through adaptation (as in Fig. 2c).

Fig. 5 plots five model saccade trajectories for each of the three distractor positions (17°, 45°, 60°; $DTOA_{0ms}$). These saccades were those resulting from the parameter value combinations with the highest probability. These results clearly illustrate the position effect: deviation away is consistently larger with a distractor at 60° compared to 45°. The close distractor condition produces saccades that deviate towards the distractor and land in the same direction. Note that the trajectories have the curved shape that is typically observed in the distractor paradigm, with initially strong deviation followed by an in-flight correction that decreases as the saccade progresses.

To investigate the latency effect, the correlation between latency and deviation was computed for the saccade populations generated with a 45° distractor paradigm. Fig. 6 illustrates these individual trial distributions. The correlation between latency and deviation was relatively strong (r = −0.697) in the $DTOA_{0ms}$ condition. Curiously, the latency effect seems to 'flatten out' for the longest latencies (>300 ms). In the model, this is the result of saturation of adaptation. Interestingly, this pattern was also found in earlier studies on the latency effect, but has never been explicitly addressed. (Mulckhuyse et al., 2009; Van der Stigchel and Theeuwes, 2005; McSorley et al., 2009b). The correlation between latency and deviation was less prominent in the $DTOA_{400ms}$ condition ($r = -0.433$), showing that our model indeed predicts that the latency effect is reduced with the $DTOA_{400ms}$.

In their study, White et al. (2012) split trials based the direction of deviation, which allows for further comparison with our model. They found that saccades deviating towards did so much less with a $DTOA_{400ms}$. Our model shows a comparable effect for the 17°-distractor simulation. For saccades deviating away, they also found that these were smaller with $DTOA_{400ms}$, which resulted on average in similar overall deviation with 0 versus 400 ms DTOA. Our simulations showed on average less deviation away with a $DTOA_{400ms}$. This is largely due to different proportions of saccades deviating towards or away from the distractor: in (White et al., 2012) the two types of saccades were approximately equal in number, so that the overall deviation balanced out in the average; in the model, saccades deviating away were much more numerous and the decreased deviation away dominated the average. Another factor might again be competition in the early visual pathway. When the distractor is presented in isolation 400 ms before target onset, it is likely to evoke a stronger response than when it has to compete with a simultaneously presented target. Indeed, model variations with stronger distractor activity in the $DTOA_{400ms}$ yielded deviation away comparable to the $DTOA_{0ms}$, while still yielding a decreased latency effect.

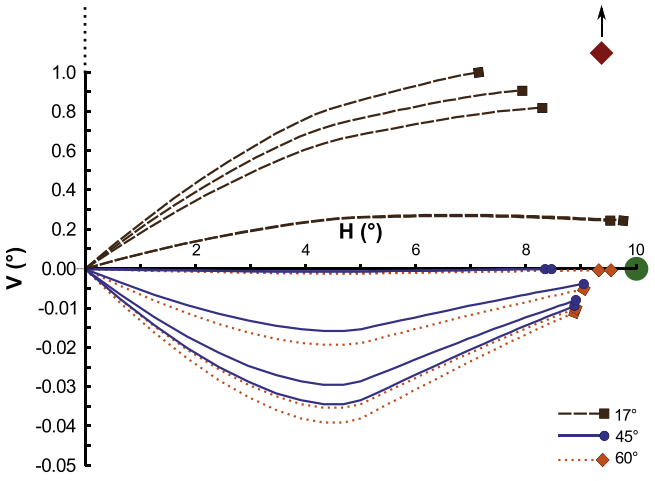

Fig. 5. Model trajectories in the $DTOA_{0\ ms}$ condition to a target at (10,0), illustrating the position effect. Five trajectories are depicted for each of the three distractor positions: close to the target (17°) and far away from the target (45° and 60°). Each distractor lies in the upper hemifield, and the parameter combinations are equal. The 17° distractor results in deviation towards and global effect, whereas both far distractor conditions yield deviation away, which is larger with a distractor at 60° than at 45°. Mind the different scales on the three axes.

4.2. Experimental results

On average 27% of all the trials with a distractor were excluded from the analysis. The primary reason for exclusion were saccades that did not land on the target (17% for $DTOA_{0ms}$ trials, and 8% for $DTOA_{400ms}$). Further analysis of these errors revealed that for $DTOA_{0ms}$, they consisted of trials that landed on the distractor (6.9%) or in between target and distractor (1.3%), trials that landed elsewhere (4.0%) and erroneously recorded trials where the measured trajectory made a large (> 2.5°) jump between samples (9.6%). The proportion of misdirected saccades was much lower with $DTOA_{400ms}$: 0.04% to the distractor, 0.2% global effect trials, 2.3% directed elsewhere (and 5.6% erroneously recorded). This difference can be readily explained from the activity profile of visual input in the model, as persistent distractor activity will be less disruptive than the transient pulse at its onset.

The primary goal of the experiment was to compare the latency effects between DTOA conditions, so producing comparable latencies was crucial. Table 2 gives an overview of latency- and deviation data. A paired sample *t*-test indeed indicated no difference between both DTOA conditions ($t(15) = 0.43$, $p = 0.67$), suggesting that the warning signal manipulation was effective.

To visualize the latency effect, trials were split into five latency bins per condition per participant. Fig. 7 shows mean latency and mean deviation for each bin, averaged over participants. In the $DTOA_{0\ ms}$ condition, average deviation tended to be towards, (similar to McSorley et al., 2009a). Saccades deviated away and towards in equal proportions (proportion away, $M = 52\%$, $SD = 6\%$, $t(15) = 1.59$, $p = 0.132$), but deviation towards was generally larger than away. Note that our criteria did not exclude potential turn-around saccades, in which deviation could be up to 45° if they were initially directed to the distractor. Analysis per bin showed that slow-latency saccades, in the last two bins, did produce reliable deviation away (One sided *t*-tests: for bin 4 $M = -0.74$, $SD = 1.87$, $t(15) = -1.59$, $p = 0.066$; for bin 5 $M = -1.73$, $SD = 1.87$, $t(15) = -3.7$, $p = 0.0011$). The simulation results presented earlier match the trend in the data, with later saccades deviating more strongly away from the distractor, although our model produces far fewer fast saccades deviating towards the distractor. This discrepancy might be caused by the warning signal in the experiment. The $DTOA_{400\ ms}$ condition produced deviation away overall ($M = -2.09$, $SD = 1.51$, $t(15) = -5.56$, $p < 0.001$), with more trials deviating away than towards (proportion away, $M = 60\%$, $SD = 5.6\%$, $t(15) = 7.1$, $p < 0.001$).

The latency effects in both conditions were compared by computing correlation coefficients (Pearson's *r*) between latency and deviation for every participant. The average correlation in the $DTOA_{0ms}$ condition was small (mean $r = -0.1289$, $SD = 0.084$) but significantly lower than zero ($t(15) = -6.16$, $p < 0.001$). With $DTOA_{400\ ms}$ the correlation was not reliably smaller than zero ($M = 0.002$, $SD = 0.068$, $t(15) = 0.11$, $p = 0.54$). A paired samples *t*-test between conditions showed that the correlation

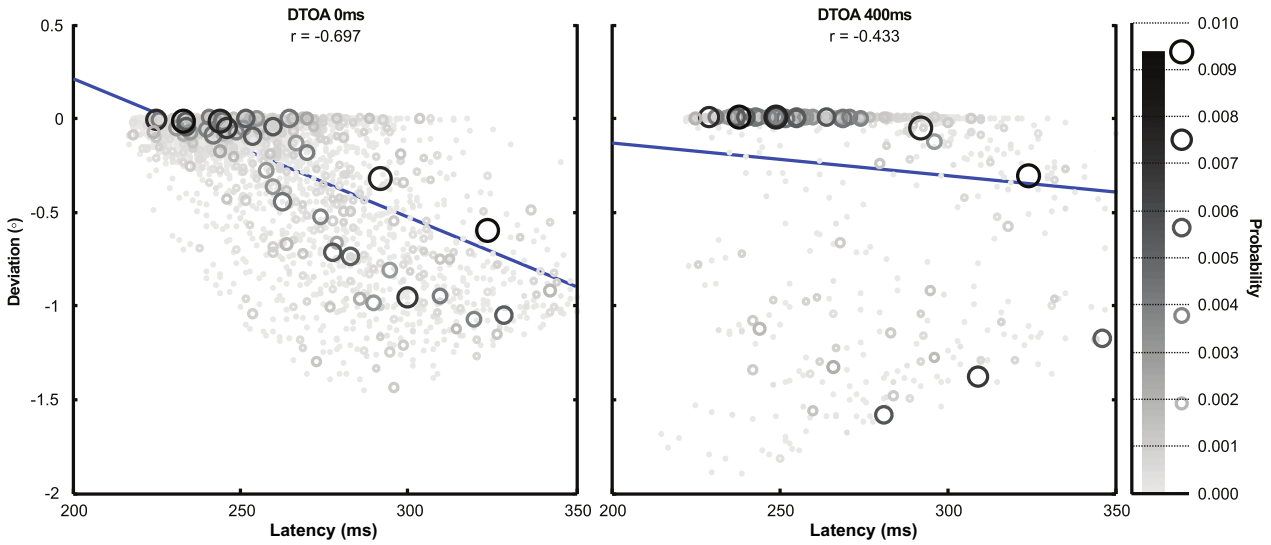

Fig. 6. Model latency and deviation in both DTOA conditions with a 45° distractor, for 25% of the parameter combinations with the highest combined probability. The shading and the relative size of data points indicates the likelihood for each trial, to visualize the distribution of the outcomes. The line represents the best-fitting regression line. The correlation (r) in the $DTOA_{0ms}$ condition is much stronger than in the $DTOA_{400\ ms}$ condition.

Table 2
Saccade deviation (in degrees) and latency (in ms) in both DTOA conditions for the two distances between target and distractor.

	$DTOA_{0\ ms}$				$DTOA_{400\ ms}$			
	Deviation		Latency		Deviation		Latency	
	M	*SD*	*M*	*SD*	*M*	*SD*	*M*	*SD*
Overall	0.22	1.7	221.2	23.1	−2.1	1.5	217.2	40.8
45°	1.54	2.4	214.3	23.3	−2.33	1.8	223.1	37.7
135°	−0.96	1.2	227.6	23.5	−1.85	1.3	211.3	44.5

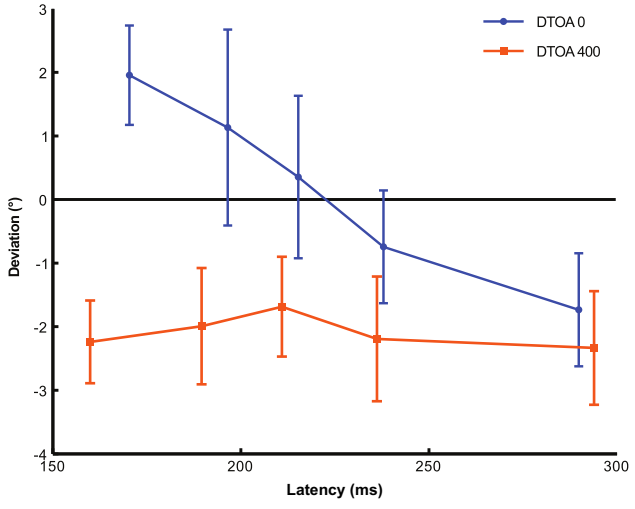

Fig. 7. Mean latency versus mean deviation within bins, averaged over all participants. Error bars indicate 95% confidence intervals. Bin data from the $DTOA_{0\ ms}$ condition clearly shows the effect of latency on deviation, whereas the $DTOA_{400ms}$ condition indicates no difference in deviation between bins.

was stronger with 0 ms DTOA that with 400 ms DTOA ($t(15) = -5.5,\ p < 0.001$), confirming the prediction of the adaptation theory.

As indicated, with $DTOA_{0ms}$ only long-latency saccades produced reliable deviation away. Therefore, the found latency effect might be explained by decreasing deviation towards, rather than increasing deviation away as in the model. Testing this explanation, we also compared the latency effect for only those saccades that deviated away. Again, this analysis confirmed our prediction: with $DTOA_{0\ ms}$ correlations (mean $r = -0.052,\ SD = 0.099$) were significantly lower than zero ($t(15) = -2.11,\ p = 0.026$) whereas for $DTOA_{400\ ms}$ (mean $r = 0.018,\ SD = 0.119$) they were not ($t(15) = 0.6,\ p = 0.723$), and again correlations were lower with 0 ms DTOA that with 400 ms DTOA ($t(15) = -1.96,\ p = 0.034$).

In the experiment, the distractor could appear at four possible locations, at 45° or 135° angular distance from the target, to prevent observers from using the distractor as a spatial cue with $DTOA_{400ms}$. Data from trials where the distractor was at 45° and at 135° were collapsed in the analyses above. We also explored results for these positions separately (Table 2), and conducted two two-way within-subjects repeated measures ANOVA's to evaluate the effects of distractor position (45° or 135°) and DTOA (0 ms or 400 ms) on deviation and latency. Saccades deviated away more with 135° distractors than with 45° distractors ($F(1,15) = 19.68,\ p < 0.001,\ \eta_p^2 = 0.567$), and more with $DTOA_{400ms}$ than with $DTOA_{0ms}$ ($F(1,15) = 11.9,\ p = 0.004,\ \eta_p^2 = 0.443$). Distractor position and DTOA also interacted ($F(1,15) = 30.9,\ p < 0.001,\ \eta_p^2 = 0.673$). Paired sample *t*-tests revealed that the interaction was caused by more deviation away for the 135° distractor than 45° with $DTOA_{0\ ms}$ ($t(15) = 5.75,\ p < 0.001$), whereas the reversed pattern approached significance with $DTOA_{400\ ms}$ ($t(15) = -2.00,\ p = 0.064$). For latencies, only the interaction DTOA × distractor position was significant ($F(1,15) = 39.03,\ p < 0.001,\ \eta_p^2 = 0.722$; both main effects $F < 1$). Here, paired *t*-tests revealed that the interaction was due to shorter latencies with a 45° distractor for $DTOA_{0\ ms}$ ($t(15) = -8.03,\ p < 0.001$), and the opposite pattern for $DTOA_{400ms}$ ($t(15) = 3.65,\ p = 0.002$).

The differences between 45°- and 135° distractors can be largely explained in terms of facilitation by the 45°-distractor, as we found in simulations with a 17° distractor. With $DTOA_{0ms}$, saccades are relatively fast and tend to deviate towards; with $DTOA_{400ms}$ they are slower and effects of deviation towards are no longer seen (compare the results of the model with 17° distractors). In contrast, 135° distractors exert no facilitating effect: with $DTOA_{0ms}$ saccades are slower and deviate away more. With $DTOA_{400ms}$, competition is resolved quickly and deviation towards the distractor is rare, which results in more deviation away overall.

4.3. General discussion

Saccade deviation away from irrelevant distractors is commonly explained by assuming a form of top-down inhibition focused at the distractor representation. However, recent findings controvert rather than support this assumption. The adaptation theory presented here offers a new perspective on how saccade deviation arises. The theory is consistent with critical findings that have given rise to the inhibition view, as well as findings disputing it. In this study, we integrated the theory into a neurocomputational model of saccade production. The model produced saccades that deviate away and towards under the conditions known from the literature and curved back towards the target as in reality. The model reproduces latency- and position effects. Moreover, the model produced a straightforward prediction: the latency effect would be absent in a $DTOA_{400ms}$ – paradigm. This prediction was subsequently confirmed by our experiment.

Underlying the adaptation theory of deviation away is the assumption that presaccadic distractor activity during target selection results in an unbalanced translation of the saccade command into a motor drive in the brainstem. We proposed that this takes place in the LLBNs, based on their connectivity (Ramat et al., 2007; White et al., 2011) and because their 'long-lead' is readily explained by such presaccadic stimulation. One could argue that the connectivity of the LLBNs is not as clear as this view suggests: for example Scudder et al. (2002) suggested that the SC directly projects to the EBNs/IBNs, without clear LLBN-involvement. Note, that this would only contradict our specific implementation, and not the adaptation theory as a whole. Faulty translation of the saccade command could, for example, be caused similarly through synaptic depletion in the SC-EBNs/IBNs projection.

To our knowledge, the only other theory of saccade deviation that does not rely on spatial inhibition of distractors was proposed in a recent modeling study (Wang et al., 2012). In their model, lateral interactions within the SC, defined by a Mexican-hat shaped kernel (cf. Trappenberg et al., 2001) caused distractor- and target activity to compete in a push–pull manner. As a result, distractor activity at the appropriate collicular distance will 'push' the target representation away. Although this theory does not require spatial inhibition, several issues arise in this scheme. First, much like inhibition theories, the lateral interaction view assumes an erroneous target representation, leaving it unanswered how corrective curvature arises in-flight. Most importantly, however, their model assumes a winner-take-all scheme to decode the SC command, neglecting the strong evidence for a distributed vector summation or averaging scheme (Goossens and Van Opstal, 2006; Gandhi and Katnani, 2011; Katnani et al., 2012; Badler and Keller, 2002; Lee et al., 1988). It is debatable whether distributed activity – not just the shifted peak – could evoke deviation away in their simulations. Sub-threshold stimulation of the SC or FEF at a location corresponding to a 90° distractor is known to result in deviation towards this location rather than away (McPeek et al., 2003; McPeek, 2006), whereas the lateral inhibition model should predict deviation away.

We highlight these model shortcomings because they are illustrative of a remarkable dissociation that has arisen in the literature on saccade generation. One class of studies, including most research on deviation away, seems to focus on target selection as controlled by the SC and upstream structures projecting to it (Wang et al., 2012; Trappenberg et al., 2001; McSorley et al., 2009a; McPeek et al., 2003), whereas another class focuses on saccade trajectories, kinematics and landing positions – associated with the downstream SC-MNs pathway in the brainstem (Robinson, 1975, chap. 24; Quaia et al., 1999; Katnani and Gandhi, 2011). Various issues with upstream theories highlighted in this article are largely related to their tacit assumption that the saccade is fully determined at the stage of the SC. Conversely, Katnani et al. (2012) recently investigated a specific model of SC-decoding. They failed to find conclusive support for this downstream model, and discussed that critical factors missing from the model were intracollicular interactions and influences from SNr or FEF – typically considered in upstream studies. The shortcomings of both classes illustrate the need for an integrated view on saccade generation. We believe our model makes a significant step towards a unified understanding of target selection and saccade production, from visual input to saccade termination. Moreover, using this integrated approach, we show that deviation away does not need to be interpreted as a sign of top down inhibition, and thereby banish one more deus ex machina from the oculomotor system.

Acknowledgments

The eye-tracking experiments were run by Astrid Heikens. This research was funded by two Grants from NWO (Netherlands organization for Scientific Research): Grant 451-09-019 to SvdS, and a VIDI Grant 452-09-007 to MM.

Appendix A. Model

A.1. Input to the SC: V1, FEF, DLPFC

V1-activity reflects exogenous stimulation, with one node for each stimulus (target, fixation or distractor). Unit activity $r_v(t)$ is described by:

$$r_v(t) = \begin{cases} S_v b\left(e^{\frac{-(t-t_{on})}{\tau_1}} - e^{\frac{-(t-t_{on})}{\tau_2}}\right), & \text{following onset} \\ S_v, & \text{persistent stimulation} \\ S_v e^{-(t-t_{off})\tau_d}, & \text{following offset} \end{cases} \quad (A.1)$$

where S_v is the strength of the stimulus (Section 2.2 and B); t_{on} and t_{off} are the time of stimulus onset and offset; time constants $\{\tau_1 = 5\text{ ms};\ \tau_2 = 6\text{ ms};\ \tau_d = 25\text{ ms}\}$ shape the fast visual onset pulse and slower decay; and scaling constant $b = 100\left(\frac{\tau_2-\tau_1}{\tau_1\tau_2}\right)$. The DLPFC modeled excitatory and inhibitory input for target and distractor, respectively. The persistent- and offset phases were defined as in Eq. A.1, using S_d instead of S_v and $\tau_d = 150$ ms, and with an assumed delayed response (t_{dl}=30 ms). DLPFC signal onset was no pulse, but a gradual increase over 50 ms:

$$r_{dlpfc}(t) = S_d \frac{t - (t_{on} + t_{dl})}{50} \quad (A.2)$$

FEF integrated the inputs, and the strength of excitatory projections between structures were mapped to the $[0, 1]$ domain using a sigmoid function:

$$e_{net} = 1 - \exp\left(\sum_k w_k e_k / c\right)^{-1} \quad (A.3)$$

where $k = \{V1, DLPFC\}$, $w = \{1, 1\}$, $c = 0.5$. FEF consisted of a single unit per stimulus, whose activity v evolved over time using:

$$\Delta v = (-(v_0 - v) + e_{net} \cdot (v_e - v) + i_{net} \cdot (v_i - v) + i_{lat} \cdot (v_i - v))/\tau \quad (A.4)$$

where $\{v_0, v_e, v_i\}$ reflect reversal potentials of the leak current, Na^+ and Cl^- (−75 mV, +30 mV, −90 mV rescaled to $\{0, 7, -1\}$ respectively) and lateral inhibition (see below); time constant $\tau = 50$ms. e_{net} And i_{net} reflected excitatory and inhibitory input, and lateral inhibition i_{lat} within FEF was computed for every node j by:

$$i_{lat,j}(t) = s_l \sum_{i \neq j}^{n} r_i(t - d) \quad (A.5)$$

where delay $d = 3$ms and scaling factor $s_l = -1$. Node output $r(t)$ was activity $v(t)$ thresholded at 67.5mV (i.e. $\theta = 0.5$).

A.2. The SC

The SC structure modeled two collicular slices as two 101×85 grids of nodes. This complies with an estimated 6 mm $\times$ 5 mm area. Nodes related to a location in visual space through the coordinate transformation of Van Gisbergen et al. (1987). Where this transformation produced locations outside of the visual field (eccentricities over 90° or locations in the ipsilateral visual field) nodes were not implemented. SC input from FEF trailed input from V1 by 10 ms. Again, inputs were transformed to the $[0, 1]$ domain using Eq. A.3, but with different input parameters $k = \{V1, FEF\}$, $w = \{0.85, 2\}$, and $c = 0.25$. Inputs innervated the corresponding SC-location via gaussian-weighted projections, for every SC-node i:

$$W_i = \exp\left(\frac{-\Delta x^2}{2\sigma^2}\right) \tag{A.6}$$

where Δx is node distance in mm and $\sigma = 0.245$. The shape the projection matched earlier estimates of movement- and visual field sizes (Trappenberg et al., 2001; Dorris et al., 2007). SC unit behavior evolved like FEF, via Eqs. A.4 and A.5 but with $\tau = 25$ ms and $s_l = 0.03$).

Distributed output activity was decomposed through vector summation (Section 2.1.2).Every node i in SC had a movement vector $\vec{v}_i$ corresponding to the associated location in visual space. Four activity values encoding four directions were computed via:

$$a_{\mathrm{x}}(t) = \sum_{i \in \mathrm{SC}} \mathrm{Max}(||r_i(t)\vec{v}_i \cdot \vec{h_{\mathrm{x}}}||, 0) \tag{A.7}$$

where $\mathrm{x} = \{\mathrm{up}, \mathrm{down}, \mathrm{left}, \mathrm{right}\}$, and $a_{\mathrm{x}}(t) \geqslant 0$.

A.3. The brainstem model: OPN, LLBN and the Cerebellum

Saccade initiation followed a simple thresholding procedure, without an explicit OPN model:

$$|a_{\mathrm{up}} - a_{\mathrm{down}}| + |a_{\mathrm{right}} - a_{\mathrm{left}}| > \theta_{\mathrm{sacc}} \tag{A.8}$$

where $\theta_{\mathrm{sacc}} = 245.0$.

Four model LLBN units determined the drive. Their behavior was computed using activity v and the internal accommodation u:

$$\begin{aligned} v_x(t) &= \tau_1 v_x(t-1) + i_x(t) \cdot (1-\tau_1) \cdot (1 - u_x(t)) \\ u_x(t) &= \mathrm{Max}(\tau_2 u_x(t-1) + c\, v_x(t-1), \beta) \end{aligned} \tag{A.9}$$

where every input $i_x(t) = \frac{a_x(t)}{100}$; temporal parameters $\tau_1 = 0.8$ and $\tau_2 = 0.99$ modeled the effect of past activity; scaling factor $c = 0.06$; and $\beta = 0.65$ modeled saturation. The resulting LLBN-activity was in the range $[0, 1.5]$.

The saccade goal $\vec{d}_{\mathrm{sc}}$ was computed as the scaled sum SC-output values:

$$\vec{d}_{\mathrm{sc}}(t) = c \sum_{\mathrm{x}} a_{\mathrm{x}}(t) \vec{h_{\mathrm{x}}} \tag{A.10}$$

where $c = 0.04$ implements scaling, and activity in opposing directions counteracts due to $\vec{h_{\mathrm{x}}}$. After initiation, two pulses $\vec{p_{\mathrm{llbn}}}$ and $\vec{p_{\mathrm{cer}}}$ determined saccade movement:

$$\Delta\vec{s}(t) = \vec{p_{\mathrm{llbn}}}(t) + \vec{p_{\mathrm{cer}}}(t) \tag{A.11}$$

$\vec{p}_{\mathrm{llbn}}(t)$ is LLBN-output $v_x(t)$, summed cf. Eq. A.10 but with $a = 0.7$. $\vec{p}_{\mathrm{cer}}(t)$ Was given by the difference between $\vec{d}_{\mathrm{sc}}$ and an extrapolated displacement with uncorrected LLBN-pulses $\vec{d}_{\mathrm{ex}}$, as in Fig. 3:

$$\begin{aligned} \vec{d}_{\mathrm{ex}}(t) &= \vec{s}(t - t_{\mathrm{eff}}) + c\vec{p}_{\mathrm{llbn}}(t) \\ \vec{p}_{\mathrm{cer}}(t) &= z(t)\frac{\vec{d}_{\mathrm{sc}}(t) - \vec{d}_{\mathrm{ex}}(t)}{c} \end{aligned} \tag{A.12}$$

Table B.3
Model parameters that were varied. $V1_{\mathrm{x}}$ or $DLPFC_{\mathrm{x}}$ mark input strengths from V1 and DLPFC, where $\mathrm{x} = \{F, T, D\}$ indicates fixation, target or distractor node respectively. Note the absence of DLPFC-projections to fixation.

Variable	Min	Max	Step	(μ, σ)
$V1_F$	0.5	0.7	0.05	(0.45, 0.3)
$V1_T$	0.8	1.2	0.05	(1.1, 0.4)
$V1_D$	0.8	1.2	0.05	(1.1, 0.4)
$DLPFC_T$	0.5	0.9	0.1	(0.8, 0.25)
$DLPFC_D$	−0.5	−0.1	0.1	(-0.45, 0.20)

where $t_{\mathrm{eff}} = 5$ms is the efferent delay, $\vec{s}(t)$ is eye position. $z(t)$ Models how cerebellar correction is not instant, but rises from 0 to 1 in 10 ms. $c = 30$ And as a result $\vec{d}_{\mathrm{ex}}$ indicates the endpoint of an uncorrected saccade after 30 ms, starting at $\vec{s}(t - t_{\mathrm{eff}})$. The saccade terminated when $\Delta\vec{s}(t) < 0.05°/_{\mathrm{ms}}$.

Appendix B. Parameters of the saccade population

The parameters for the probability distribution described in Section 2.2 are detailed in Table B.3. The probabilities assigned to each parameter step were defined by the normal cumulative distribution function over that step, defined by μ and σ for that parameter.

References

Arai, K., Keller, E., & Edelman, J. (1994). Two-dimensional neural network model of the primate saccadic system. *Neural Networks, 7*, 1115–1135.

Badler, J., & Keller, E. (2002). Decoding of a motor command vector from distributed activity in superior colliculus. *Biological Cybernetics, 86*, 179–189.

Barlow, H. (1961). Possible principles underlying the transformation of sensory messages. *Sensory Communication*, 217–234.

Basso, M., & Wurtz, R. (2002). Neuronal activity in Substazntia nigra pars reticulata during target selection. *The Journal of Neuroscience, 22*, 1883–1894.

Bell, A., Meredith, M., Van Opstal, A., & Munoz, D. (2006). Stimulus intensity modifies saccadic reaction time and visual response latency in the superior colliculus. *Experimental Brain Research, 174*, 53–59.

Brown, J., Bullock, D., & Grossberg, S. (2004). How laminar frontal cortex and basal ganglia circuits interact to control planned and reactive saccades. *Neural Networks, 17*, 471–510.

Coren, S., & Hoenig, P. (1972). Effect of non-target stimuli upon length of voluntary saccades. *Perceptual and Motor Skills, 34*, 499–508.

Dick, S., Ostendorf, F., Kraft, A., & Ploner, C. (2004). Saccades to spatially extended targets: The role of eccentricity. *Neuroreport, 15*, 453–456.

Dorris, M., Olivier, E., & Munoz, D. (2007). Competitive integration of visual and preparatory signals in the superior colliculus during saccadic programming. *The Journal of Neuroscience, 27*, 5053–5062.

Doyle, M., & Walker, R. (2001). Curved saccade trajectories: Voluntary and reflexive saccades curve away from irrelevant distractors. *Experimental Brain Research, 139*, 333–344.

Edelman, J., & Keller, E. (1998). Dependence on target configuration of express saccade-related activity in the primate superior colliculus. *Journal of Neurophysiology, 80*, 1407–1426.

Everling, S., Paré, M., Dorris, M., & Munoz, D. (1998). Comparison of the discharge characteristics of brain stem omnipause neurons and superior colliculus fixation neurons in monkey: Implications for control of fixation and saccade behavior. *Journal of Neurophysiology, 79*, 511–528.

Evinger, C., Kaneko, C., & Fuchs, A. (1982). Activity of omnipause neurons in alert cats during saccadic eye movements and visual stimuli. *Journal of Neurophysiology, 47*, 827–844.

Ferraina, S., Paré, M., & Wurtz, R. H. (2002). Comparison of cortico-cortical and cortico-collicular signals for the generation of saccadic eye movements. *Journal of Neurophysiology, 87*, 845–858.

Gandhi, N., & Katnani, H. (2011). Motor functions of the superior colliculus. *Annual Review of Neuroscience, 34*, 205–231.

Gandhi, N., & Keller, E. (1997). Spatial distribution and discharge characteristics of superior colliculus neurons antidromically activated from the omnipause region in monkey. *Journal of Neurophysiology, 78*, 2221–2225.

Gandhi, N., & Keller, E. (1999). Comparison of saccades perturbed by stimulation of the rostral superior colliculus, the caudal superior colliculus, and the omnipause neuron region. *Journal of Neurophysiology, 82*, 3236–3253.

Gawne, T., & Martin, J. (2002). Responses of primate visual cortical neurons to stimuli presented by flash, saccade, blink, and external darkening. *Journal of Neurophysiology, 88*, 2178–2186.

Glimcher, P., & Sparks, D. (1993). Representation of averaging saccades in the superior colliculus of the monkey. *Experimental Brain Research, 95*, 429–435.

Godijn, R., & Theeuwes, J. (2002). Programming of endogenous and exogenous saccades: Evidence for a competitive integration model. *Journal of Experimental Psychology: Human Perception and Performance, 28*, 1039–1054.
Godijn, R., & Theeuwes, J. (2004). The relationship between inhibition of return and saccade trajectory deviations. *Journal of Experimental Psychology: Human Perception and Performance, 30*, 538–554.
Goossens, H., & Van Opstal, A. (2006). Dynamic ensemble coding of saccades in the monkey superior colliculus. *Journal of Neurophysiology, 95*, 2326–2341.
Handel, A., & Glimcher, P. (2000). Contextual modulation of substantia nigra pars reticulata neurons. *Journal of Neurophysiology, 83*, 3042–3048.
Hikosaka, O., Takikawa, Y., & Kawagoe, R. (2000). Role of the basal ganglia in the control of purposive saccadic eye movements. *Physiological Reviews, 80*, 953–978.
Izhikevich, E. (2003). Simple model of spiking neurons. *IEEE Transactions on Neural Networks, 14*, 1569–1572.
Jantz, J. J., Watanabe, M., Everling, S., & Munoz, D. P. (2013). Threshold mechanism for saccade initiation in frontal eye field and superior colliculus. *Journal of Neurophysiology, 109*, 2767–2780.
Jiang, H., Stein, B., McHaffie, J., et al. (2003). Opposing basal ganglia processes shape midbrain visuomotor activity bilaterally. *Nature, 423*, 982–986.
Johnston, K., & Everling, S. (2006). Neural activity in monkey prefrontal cortex is modulated by task context and behavioral instruction during delayed-match-to-sample and conditional prosaccade antisaccade tasks. *Journal of Cognitive Neuroscience, 18*, 749–765.
Kalesnykas, R., & Hallett, P. (1994). Retinal eccentricity and the latency of eye saccades. *Vision Research, 34*, 517–531.
Kaneko, C. (2006). Saccade-related, long-lead burst neurons in the monkey rostral pons. *Journal of Neurophysiology, 95*, 979–994.
Katnani, H., & Gandhi, N. (2011). Order of operations for decoding superior colliculus activity for saccade generation. *Journal of Neurophysiology, 106*, 1250–1259.
Katnani, H., van Opstal, A., & Gandhi, N. (2012). A test of spatial temporal decoding mechanisms in the superior colliculus. *Journal of Neurophysiology*.
Kusunoki, M., Gottlieb, J., & Goldberg, M. (2000). The lateral intraparietal area as a salience map: The representation of abrupt onset, stimulus motion, and task relevance. *Vision Research, 40*, 1459–1468.
Lee, C., Rohrer, W., Sparks, D., et al. (1988). Population coding of saccadic eye movements by neurons in the superior colliculus. *Nature, 332*, 357–360.
Ludwig, C., & Gilchrist, I. (2003). Target similarity affects saccade curvature away from irrelevant onsets. *Experimental Brain Research, 152*, 60–69.
Lui, F., Gregory, K., Blanks, R., & Giolli, R. (1995). Projections from visual areas of the cerebral cortex to pretectal nuclear complex, terminal accessory optic nuclei, and superior colliculus in macaque monkey. *The Journal of Comparative Neurology, 363*, 439–460.
Marino, R., Rodgers, C., Levy, R., & Munoz, D. (2008). Spatial relationships of visuomotor transformations in the superior colliculus map. *Journal of Neurophysiology, 100*, 2564–2576.
McPeek, R. (2006). Incomplete suppression of distractor-related activity in the frontal eye field results in curved saccades. *Journal of Neurophysiology, 96*, 2699–2711.
McPeek, R., Han, J., & Keller, E. (2003). Competition between saccade goals in the superior colliculus produces saccade curvature. *Journal of Neurophysiology, 89*, 2577–2590.
McSorley, E., Cruickshank, A., & Inman, L. (2009a). The development of the spatial extent of oculomotor inhibition. *Brain Research, 1298*, 92–98.
McSorley, E., Haggard, P., & Walker, R. (2004). Distractor modulation of saccade trajectories: Spatial separation and symmetry effects. *Experimental Brain Research, 155*, 320–333.
McSorley, E., Haggard, P., & Walker, R. (2006). Time course of oculomotor inhibition revealed by saccade trajectory modulation. *Journal of Neurophysiology, 96*, 1420–1424.
McSorley, E., Haggard, P., & Walker, R. (2009b). The spatial and temporal shape of oculomotor inhibition. *Vision Research, 49*, 608–614.
Meeter, M., Myers, C., & Gluck, M. (2005). Integrating incremental learning and episodic memory models of the hippocampal region. *Psychological Review, 112*, 560–585.
Meeter, M., Van der Stigchel, S., & Theeuwes, J. (2010). A competitive integration model of exogenous and endogenous eye movements. *Biological Cybernetics, 102*, 271–291.
Mulckhuyse, M., Van der Stigchel, S., & Theeuwes, J. (2009). Early and late modulation of saccade deviations by target distractor similarity. *Journal of Neurophysiology, 102*, 1451–1458.
Munoz, D. (2002). Commentary: Saccadic eye movements: Overview of neural circuitry. *Progress in Brain Research, 140*, 89–96.
Munoz, D., Dorris, M., Pare, M., & Everling, S. (2000). On your mark, get set: Brainstem circuitry underlying saccadic initiation. *Canadian Journal of Physiology and Pharmacology, 78*, 934–944.
Munoz, D., & Istvan, P. (1998). Lateral inhibitory interactions in the intermediate layers of the monkey superior colliculus. *Journal of Neurophysiology, 79*, 1193–1209.
Munoz, D., & Schall, J. (2004). Concurrent, distributed control of saccade initiation in the frontal eye field and superior colliculus. In W. Hall & A. Moschovakis (Eds.), *The superior colliculus: New approaches for studying sensorimotor integration chapter 3* (pp. 55–82). CRC Press.
Optican, L., & Robinson, D. (1980). Cerebellar-dependent adaptive control of primate saccadic system. *Journal of Neurophysiology, 44*, 1058–1076.
Postle, B. (2006). Working memory as an emergent property of the mind and brain. *Neuroscience, 139*, 23–38.
Quaia, C., Lefèvre, P., & Optican, L. (1999). Model of the control of saccades by superior colliculus and cerebellum. *Journal of Neurophysiology, 82*, 999–1018.
Ramat, S., Leigh, R., Zee, D., & Optican, L. (2007). What clinical disorders tell us about the neural control of saccadic eye movements. *Brain, 130*, 10–35.
Rizzolatti, G., Riggio, L., Dascola, I., & Umiltá, C. (1987). Reorienting attention across the horizontal and vertical meridians: Evidence in favor of a premotor theory of attention. *Neuropsychologia, 25*, 31–40.
Robinson, D. (1972). Eye movements evoked by collicular stimulation in the alert monkey. *Vision Research, 12*, 1795–1808.
Robinson, D. (1975). Oculomotor control signals. In B. Lennerstrand & P. Bach-y Rita (Eds.), *Basic mechanisms of ocular motility and their clinical implications* (pp. 337–374). Oxford: Pergamon Press.
Rodgers, C., Munoz, D., Scott, S., & Paré, M. (2006). Discharge properties of monkey tectoreticular neurons. *Journal of Neurophysiology, 95*, 3502–3511.
Rucker, J., Ying, S., Moore, W., Optican, L., Büttner-Ennever, J., Keller, E., et al. (2011). *Do brainstem omnipause neurons terminate saccades?* Annals of the New York Academy of Sciences.
Schlag-Rey, M., Schlag, J., & Dassonville, P. (1992). How the frontal eye field can impose a saccade goal on superior colliculus neurons. *Journal of Neurophysiology, 67*, 1003–1005.
Scudder, C., Kaneko, C., & Fuchs, A. (2002). The brainstem burst generator for saccadic eyemovements. *Experimental Brain Research, 142*, 439–462.
Scudder, C., Moschovakis, A., Karabelas, A., & Highstein, S. (1996). Anatomy and physiology of saccadic long-lead burst neurons recorded in the alert squirrel monkey. I. Descending projections from the mesencephalon. *Journal of Neurophysiology, 76*, 332–352.
Sheliga, B., Riggio, L., & Rizzolatti, G. (1994). Orienting of attention and eye movements. *Experimental Brain Research, 98*, 507–522.
Sommer, M., & Wurtz, R. (2000). Composition and topographic organization of signals sent from the frontal eye field to the superior colliculus. *Journal of Neurophysiology, 83*, 1979–2001.
Sparks, D. et al. (2002). The brainstem control of saccadic eye movements. *Nature Reviews Neuroscience, 3*, 952–964.
Theeuwes, J., Belopolsky, A., & Olivers, C. (2009). Interactions between working memory, attention and eye movements. *Acta Psychologica, 132*, 106–114.
Tinsley, C., & Everling, S. (2002). Contribution of the primate prefrontal cortex to the gap effect. *Progress in Brain Research, 140*, 61–72.
Trappenberg, T., Dorris, M., Munoz, D., & Klein, R. (2001). A model of saccade initiation based on the competitive integration of exogenous and endogenous signals in the superior colliculus. *Journal of Cognitive Neuroscience, 13*, 256–271.
Van der Stigchel, S. (2010). Recent advances in the study of saccade trajectory deviations. *Vision Research, 50*, 1619–1627.
Van der Stigchel, S., Meeter, M., & Theeuwes, J. (2006). Eye movement trajectories and what they tell us. *Neuroscience & Biobehavioral Reviews, 30*, 666–679.
Van der Stigchel, S., Meeter, M., & Theeuwes, J. (2007). The spatial coding of the inhibition evoked by distractors. *Vision Research, 47*, 210–218.
Van der Stigchel, S., & Nijboer, T. (2011). The global effect: What determines where the eyes land. *Journal of Eye Movement Research, 4*, 1–13.
Van der Stigchel, S., & Theeuwes, J. (2005). Relation between saccade trajectories and spatial distractor locations. *Cognitive Brain Research, 25*, 579–582.
Van der Stigchel, S., & Theeuwes, J. (2006). Our eyes deviate away from a location where a distractor is expected to appear. *Experimental Brain Research, 169*, 338–349.
Van Gisbergen, J., Robinson, D., & Gielen, S. (1981). A quantitative analysis of generation of saccadic eye movements by burst neurons. *Journal of Neurophysiology, 45*, 417–442.
Van Gisbergen, J., Van Opstal, A., & Tax, A. (1987). Collicular ensemble coding of saccades based on vector summation. *Neuroscience, 21*, 541–555.
Van Opstal, A., & Goossens, H. (2008). Linear ensemble-coding in midbrain superior colliculus specifies the saccade kinematics. *Biological Cybernetics, 98*, 561–577.
Walker, R., Deubel, H., Schneider, W., & Findlay, J. (1997). Effect of remote distractors on saccade programming: Evidence for an extended fixation zone. *Journal of Neurophysiology, 78*, 1108–1119.
Walker, R., & McSorley, E. (2008). The influence of distractors on saccade target selection: Saccade trajectory effects. *Journal of Eye Movement Research, 2*, 1–9.
Wang, Z., Kruijne, W., & Theeuwes, J. (2012). Lateral interactions in the superior colliculus produce saccade deviation in a neural field model. *Vision Research, 62*, 66–74.
White, B., & Munoz, D. (2011). The superior colliculus. In S. Liversedge, I. Gilchrist, & S. Everling (Eds.), *Oxford handbook of eye movements* (pp. 195–213). New York: Oxford University Press.
White, B., Theeuwes, J., & Munoz, D. (2012). Interaction between visual-and goal-related neuronal signals on the trajectories of saccadic eye movements. *Journal of Cognitive Neuroscience, 24*, 707–717.